Scientific paper

Quality by Design Based Development of Electrospun Nanofibrous Solid Dispersion Mats for Oral Delivery of Efavirenz

Md. Faseehuddin Ahmed,^{1,2} Kalpana Swain,¹ Satyanarayan Pattnaik¹ and Biplab Kumar Dey^{2,*}

¹ Talla Padmavathi College of Pharmacy, Warangal, India

² Faculty of Pharmaceutical Sciences, Assam Down town University, Guwahati, Assam, India

* Corresponding author: E-mail: drbiplabdey9@gmail.com Mobile-+91-7386752617

Received: 11-14-2023

Abstract

Poor aqueous solubility often results in poor dissolution behavior and, consequently, poor bioavailability for those drugs whose intestinal absorption is dissolution rate limited. It is essential for formulation scientists to identify strategies to improve the solubility and dissolution rate of candidate drugs in order to improve their bioavailability. The present study investigated electrospun polymeric nanofibers for efavirenz (an antiretroviral drug), a Class II drug in the Biopharmaceutical Classification System. In order to fabricate nanofibers, hydrophilic spinnable polymer like Soluplus was used. Statistical design of experiments was used to optimize electrospinning parameters. Scanning electron microscopy (SEM) studies confirmed the presence of nanofibrous material in the mat. The x-ray diffraction (XRD) and differential scanning calorimetry (DSC) studies advocated the amorphization of efavirenz in the nanofiber samples. The optimized nanofiber-based platform significantly improved in vitro dissolution of efavirenz (89.0 \pm 3.2% in 120 minutes) compared to pure efavirenz crystals (27.3 \pm 2.4%).

Keywords: Electrospinning; Nanomedicine; Bioavailability; Absorption; Efavirenz

1. Introduction

The recent past has witnessed tremendous efforts to develop new chemical entities with promising therapeutic efficacy via artificial intelligence tools.^{1,2} Though the drug candidates exhibited desired therapeutic response during pharmacological screening, many could not reach the market due to poor oral bioavailability which is mostly due to poor aqueous solubility, poor intestinal permeability, or both.³⁻⁷ The effective and optimal therapeutic outcomes of drugs are often related to the availability of the drug in sufficient quantity at the desired site of action. The rate-limiting step for the drugs which exhibit poor soluble but good permeability is the dissolution in biological fluids in vivo. Most of the recently developed drug candidates suffer from the issues of poor solubility and hence the pharmaceutical industry and researchers across the world are seeking a viable solution to this challenge.

In this scenario, nanotechnology has offered some wonderful platform technologies for improving the oral bioavailability of drug substances. 8-17 Various nanotechnology-based solutions to improve oral bioavailability, via solubilization of candidate drugs, include nanocrystals, nanomorphs, nanosuspensions, nanocapsules, lipid-based nanoparticles, dendrimers, polymeric nanocarriers, amorphous solid nanodispersions, nanofibers, etc.

Amorphous product development has become a common choice for enhancing the solubility of poorly soluble pharmaceutical compounds. In these cases, the crystalline lattice of the drug substance undergoes disruption, leading to a higher energy state in the amorphous form, thereby improving solubility. The role of polymers in the development of amorphous products includes stabilizing the amorphous system through the prevention of devitrification and ensuring improved physical stability under various accelerated conditions, such as elevated temperature and relative humidity. In comparison to other documented solubilization methods, amorphous solid dispersions are particularly favored for low-solubility drugs. The sus-

tained supersaturation of these products in the gastrointestinal tract contributes to the enhanced bioavailability of the drug. Controlled supersaturation allows for increased drug absorption compared to conditions where a saturated solution is maintained.

Though solid dispersion technology has tremendous capabilities to formulate amorphous drug products, stability issues related to devitrification remain a key challenge. Hot melt extrusion technology as a method of developing amorphous solid dispersion has numerous benefits but limits the processing of thermolabile substances. In this situation, nanofiber technology may be a viable solution to develop amorphous solid dispersions of candidate drugs. Electrospinning is a manufacturing method employed for the creation of extremely fine fibers, generally within the nanometer to micrometer scale. This procedure entails applying an electric field to either a polymer solution or melt, leading the material to be pulled into fine fibers due to the influence of electrostatic forces. The outcome is the formation of a nonwoven mat or membrane composed of these fibers. 11 Electrospinning generates a potent amorphization effect because the solvent evaporates instantly, leading to a solid solution of the drug in the polymer matrix. 11,15,18 Due to the uniform distribution of the cargo molecules inside the polymer matrix and possible inhibition of molecular mobility leading to impaired devitrification, the amorphous state of the loaded therapeutic ingredient is preserved for longer in the solid dispersions fabricated via electrospinning. Electrospinning for the fabrication of drug-loaded nanofibers has been exploited by researchers across the world for multiple purposes including attempts to improve oral bioavailability and controlled / sustained drug delivery. 19-21 Recently, from our laboratory, we have reported improved in-vitro dissolution and ex-vivo intestinal permeation of ibuprofen (a poorly soluble drug) utilizing the nanofiber technology.15

An amphiphilic polymeric solubilizer, Soluplus[®] is a polycaprolactam-polyvinylacetate-polyethylene glycol graft copolymer (Figure 1). The creation of solid solutions using Soluplus can significantly increase the solubility of poorly soluble pharmaceuticals in aqueous media because of its outstanding solubilizing properties for Biopharmaceutical Classification System (BCS) class II drugs.²² The Biopharmaceutics Classification System (BCS) serves as a framework for classifying drugs based on their solubility and permeability characteristics. It consists of four classes: Class I, II, III, and IV. Class I drugs demonstrate both high solubility and permeability, leading to enhanced bioavailability. Conversely, Class II drugs have high permeability but low solubility, presenting challenges to bioavailability due to incomplete dissolution. Class III drugs possess high solubility but low permeability, potentially restricting absorption. In contrast, Class IV drugs, characterized by low solubility and permeability, encounter obstacles in both dissolution and absorption processes.

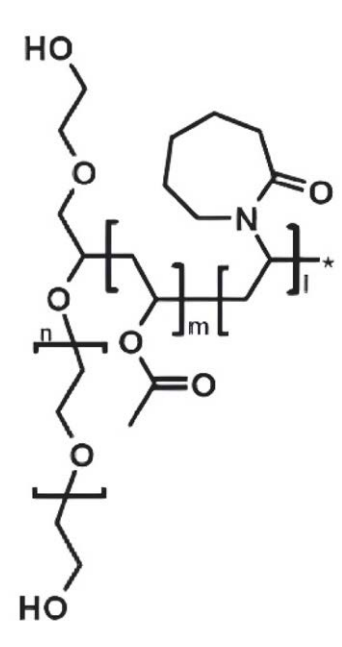


Figure 1. Chemical structure of Soluplus.

This matrix-forming polymer is quite prevalent, and because they are effective solubilizers, they have long been employed to create solid dispersions. Though, a few attempts were reported to prepare Soluplus*-based nanofiber, an experimentally designed approach for optimization of formulation and process variables is lacking.²³

Non-nucleoside reverse transcription inhibitors (NNRTIs) have been widely used in antiretroviral cocktails as a part of highly active antiretroviral therapy (HAART). Efavirenz (EFV) is commonly prescribed NNRTI and has shown significant therapeutic benefits by lowering the viral load in patients with HIV infection (Figure 2).²⁴ However, the drug belongs to BCS class II exhibiting poor aqueous solubility and high intestinal permeability. Subsequently, EFV exhibits a low intrinsic dissolution rate (0.037 mg/cm²/min), and poor oral bioavailability (40-50%).²⁴ Such BCS class II drugs where drug dissolution is the rate-limiting step in overall oral drug absorption, strategies to improve aqueous solubility is a promising approach for improvement in oral bioavailability.²⁵ Hence, there is a strong motivation to improve the dissolution velocity of EFV.

An electrospinning approach was explored in the present study to amorphize EFV to improve its aqueous solubility and oral bioavailability. Nanofibers were characterized by scanning electron microscopy (SEM), X-ray diffraction (XRD), and differential scanning calorimeter (DSC). The results showed that EFV was successfully amorphized and converted into nanofibers.

2. Materials and Methods

2. 1. Materials

Efavirenz (EFV) was obtained as a gift sample from Cipla Ltd (Mumbai, India). Soluplus* (polyvinyl caprolactam-polyvinyl acetate-polyethylene glycol graft co-polymer; CAS Number-402932-23-4) was obtained as a gift sample from BASF Corporation, New Jersey. Ethanol (analytical grade) was obtained from Sigma-Aldrich Corp (India). All other chemicals used were of analytical grade and procured locally.

1. 2. Development of Nanofibers

2. 2. 1. Design of Experiments (DoE)

Statistical design of experiment (DoE) was used for the development of electrospun nanofibers.^{26–29} Diverse factors which include electrospinning setup variables, working fluid variables, and ambient variables, influence the electrospinning process for the fabrication of polymeric nanofibers.11 Hence, there is a need for optimization of these variables during development. A response surface randomized Box-Behnken quadratic design with 17 runs was deployed for product development. Three important variables i.e., DC voltage, flow rate, and polymer concentration, are studied at three levels and are coded as -1(low), 0(moderate), and +1(high). The DC voltage was varied at 10kV (-1), 14kV (0), and 18 kV (+1). The flow rate was varied at 0.4 ml/h (-1), 0.8 ml/h (0), and 1.2 ml/h(+1). The Soluplus concentration was also varied at three levels i.e., 45% w/w (-1), 50% w/w (0), and 55% w/w (+1). The cumulative percent of drug released was measured for each run as a dependent response. Design-Expert[®] software (Version-13; Stat-Ease, Inc., Minneapolis) was used to generate and process the design. The nanofiber formulation with maximum drug dissolution (at 120 minutes) was selected as the optimized product for further characterization.

2. 2. 2. Fabrication of Nanofibers

Electrospinning equipment (Super ES 2; E-Spin Nanotech, India) was used for the preparation of the nanofiber mats. The electrospinning setup includes a high-voltage DC supply (up to 50kV), and a syringe pump to control the volumetric flow rate of the working solution with the option to control the temperature and humidity of the

electrospinning chamber. The electrospinning solution consisted of Soluplus* with efavirenz in ethanol (Table 1). The concentration of EFV was fixed for all the runs, but the concentration of Soluplus* varied from 45 to 55% w/w. The stated amount of EFV was initially dissolved in ethanol and subsequently, the drug was dissolved in the polymer solution. According to the Box-Behnken design, electrospinning was carried out at an applied DC voltage of 10, 14, or 18 kV with a volumetric flow rate of 0.4, 0.8, or 1.2 ml/h and spinneret to collector distance of 12 cm (Table 1).

The application of high voltages, usually within the kilovolt range, carries the potential for electrical shock hazards. Consequently, measures were taken to guarantee the proper grounding of equipment before initiating operations, and strict adherence to safety protocols, including the use of suitable personal protective equipment (PPE), was maintained when working with high voltages.

2. 3. Drug Entrapment Efficiency (EE)

The efficiency of efavirenz entrapment in the fabricated nanofiber mats was assessed as follows.

EE (%) = (EFV content measured in the sample/Actual amount of EFV added) \times 100 %

All tests were repeated in triplicate and the mean is reported. Dissolving the generated fibers in ethanol allowed the amount of efavirenz in them to be determined. To assess the amount of efavirenz in each sample, the solutions were spectrophotometrically analyzed at 248 nm.³⁰

Table 1. Experimental runs for fabrication of efavirenz loaded nanofibers following Box-Behnken design. Voltage (kV): 10 (-1), 14 (0), 18 (+1); Flow Rate (ml/h): 0.4 (-1), 0.8 (0); 1.2 (+1); Soluplus conc (% w/w): 45 (-1), 50 (0), 55 (+1). The numbers inside the parentheses (-1, 0, +1) indicate the levels of the variable (low, moderate, and high).

Run	Voltage (kV)	Flow Rate (ml/h)	Soluplus Conc (%)	Cumulative Percent Drug Released (CPD) (%)
F1	0 (14)	-1(0.4)	1(55)	79.28
F2	0(14)	0(0.8)	0(50)	89.45
F3	-1(10)	-1(0.4)	0(50)	75.22
F4	1(18)	0(0.8)	-1(45)	82.43
F5	-1(10)	0(0.8)	1(55)	65.74
F6	-1(10)	1(1.2)	0(50)	65.82
F7	0(14)	1(1.2)	-1(45)	80.16
F8	1(18)	1(1.2)	0(50)	69.84
F9	0(14)	1(1.2)	1(55)	78.52
F10	-1(10)	0(0.8)	-1(45)	77.59
F11	1(18)	0(0.8)	1(55)	64.52
F12	0(14)	-1(0.4)	-1(45)	82.18
F13	1(18)	-1(0.4)	0(50)	64.13

2.4. In Vitro Dissolution Studies

As part of the dissolution study, samples of naive efavirenz (100 mg) or nanofiber samples equivalent to 100 mg EFV were loaded into hard gelatin capsules and tied to paddles. We used 900 ml of 0.2% sodium lauryl sulfate (SLS) in 0.1 N HCl as dissolution media and the study was carried out under sink conditions. Spectrophotometric analyses of the samples at 248 nm were performed at predetermined intervals for 120 minutes following any removal of the solution, filtering, and subsequently analyzing the data using the UV-160 (Shimadzu, Japan) spectrophotometer. It was necessary to replace the same amount of medium at the same temperature to maintain the sink condition. At least three repetitions were used to calculate the average of the experimental points. The nanofiber sample that demonstrated the highest drug release underwent additional characterization using Scanning electron microscopy, differential scanning calorimetry, and x-ray diffractometry.

2. 5. Scanning Electron Microscopy (SEM)

Using the S-3700N scanning electron microscope (Hitachi, Okinawa, Japan), fiber morphology and diameter were examined. A sputter coater was used to coat samples with gold at 20 nm under vacuum. An acceleration voltage of 5 kV was used for all micrographs. Everhart-Thornley detectors were used to detect secondary electrons. An adequate number of measurement points in the image were manually determined to assess the diameter of the nanofibers after a careful calibration of the instrument for size determination

2. 6. X-ray Diffraction Studies

The X-ray diffractometer uses X-rays to fire at the samples and then analyzes diffracted patterns. It is possible to determine the crystallinity of samples by measuring their diffracted patterns. Diffractometer parameters such as voltage, current, and angular range are optimized to accurately assess crystallinity. A Panalytical X'Pert Pro X-ray diffractometer (Model: Panalytical, X'Pert Pro, UK) was used to evaluate the crystallinity of the optimized nanofiber sample and native EFV sample using nickel-filtered Cu Ka radiation (k = 1.54 A). During the measurement, the voltage and current were 35 kV and 30 mA, respectively, and were smoothed to 95. Measurements were carried out in the angular range from 6° to 50° (20) using step sizes 0.02 and 0.01s per step.

2. 7. Differential Scanning Calorimetry

Differential scanning calorimetry (DSC 3+, Mettler Toledo) was used to study the thermal behavior of native EFV and drug-loaded optimized nanofibers. Through this technique, the researchers were able to measure the

amount of heat released or absorbed when the nanofibers underwent a physical or chemical change. It allowed them to determine how the nanofibers would respond to changes in temperature and characterize their thermal behavior. Approximately 5 mg of powdered sample was placed in an aluminum pan (40 μL standard aluminum crucible with pierced lid), making sure that the crucible base and the pan surface were uniformly in contact. The pan was sealed and heated to 200 degrees Celsius at a temperature ramp rate of 10 degrees Celsius per minute under nitrogen gas (40 ml/min). A five-minute equilibration period was followed by each measurement of samples at 30 °C. For each peak, Mettler Toledo software calculated the transition temperatures and enthalpies.

2. Results and Discussions

2. 1. Design of Experiments (DoE)

Quality by Design (QbD), is a systematic approach to pharmaceutical development that is used to ensure the quality of pharmaceutical products. It is a proactive approach that focuses on building quality into the product from the beginning rather than relying on quality testing at the end of the manufacturing process. DoE (Design of Experiments) is a statistical method used in QbD to systematically explore and optimize process parameters and their interactions. By using DOE, manufacturers can identify the most critical process parameters and their optimal settings to achieve the desired quality objectives. The principles of DoE have been widely deployed by pharmaceutical researchers for the development and optimization of drug products.^{28,29} The present study adopted a Box-Behnken study design and the data were fitted to a quadratic model. The critical electrospinning variables like DC voltage, working fluid flow rate, and Soluplus concentration was chosen and varied at three levels to assess their influence on the dependent response (Table 1). The sequential model sum of squares selects the highest-order polynomial where the terms are significant and the model is not aliased. ²⁹ Here the cubic model was aliased and hence quadratic model was selected. Further, the model summary statistics indicate that the quadratic model was suitable for analyzing the dependent response. Interested readers are invited to refer to the supplementary material available in Appendix 1 for the sequential model sum of squares and model summary statistics information.

The equation in coded values generated for the quadratic model is as follows.

Cumulative percent drug released (CPD) = +89.45- 0.4312A -0.8087 B -4.29 C+3.78 AB -1.52 AC+0.3150 BC -14.08 A²-6.62 B² -2.80 C²

The coded factors A, B, and C represent DC voltage, flow rate, and Soluplus concentration, respectively. The equation in terms of coded factors can be used to make predictions about the response for given levels of each fac-

tor. By default, the high levels of the factors are coded as +1 and the low levels are coded as -1.

To assess the significance of the model terms, an analysis of variance (ANOVA) was performed. The F-Values and p-values were monitored for the purpose of identifying the significant model terms (Table 2). The Model F-value of 11.18 implies the model is significant. There is only a 0.22% chance that an F-value this large could occur due to noise. p-values less than 0.0500 indicate model terms are significant. In this case, C, A², B² are significant model terms (Table 2). Values greater than 0.1000 indicate the model terms are not significant.²⁵ The coded equation is useful for identifying the relative impact of the factors by comparing the factor coefficients. The factor coefficients are presented in Table 3. The coefficient estimate represents the expected change in response per unit change in factor value when all remaining factors are held constant. The intercept in an orthogonal design is the overall average response of all the runs. The coefficients are adjustments around that average based on the factor settings. The higher the absolute value of the coefficient estimate the higher the influence of the factor on the dependent response.

In the present case, the highest estimate was observed for Soluplus concentration followed by flow rate and voltage indicating the predominant impact of Soluplus concentration on the dependent response, i.e., cumulative percent drug released (Table 3). This is also evident from the 3d surface plot represented in Fig 3.

3. 2. Drug Entrapment Efficiency

The loading of drugs into drug delivery systems is one of the most important factors to consider when evaluating the suitability of drug carrier systems. In addition to blending (in which the drug is dissolved or dispersed in a polymer solution), surface modification (in which the drug is conjugated to the nanofiber surface), coaxial processing (co-electrospinning of a drug solution as the core and a polymer solution as the sheath), etc, there are several other ways in which drugs can be loaded into polymeric nanofibers. ^{11,31} For the loading of efavirenz in the present study, the blending method was used. The efavirenz loading efficiency in the fabricated electrospun nanofibers was as high as $98.4 \pm 4.2\%$ w/w.

Table 2. ANOVA for Quadratic model.

Source	Sum of Squares	df	Mean Square	F-value	p-value
Model	1349.89	9	149.99	11.18	0.0022
A-Voltage	1.49	1	1.49	0.1109	0.7489
B-Flow rate	5.23	1	5.23	0.3901	0.5521
C-Soluplus Conc	147.06	1	147.06	10.96	0.0129
AB	57.08	1	57.08	4.26	0.0780
AC	9.18	1	9.18	0.6845	0.4353
BC	0.3969	1	0.3969	0.0296	0.8683
A^2	834.87	1	834.87	62.24	< 0.0001
B^2	184.31	1	184.31	13.74	0.0076
C^2	32.98	1	32.98	2.46	0.1609
Residual	93.89	7	13.41		
Lack of Fit	93.89	3	31.30		
Pure Error	0.0000	4	0.0000		
Cor Total	1443.79	16			

Table 3. Coefficient estimates in Terms of Coded Factors.

Factor	Coefficient Estimate	df	Standard Error	95 % CI Low	95 % CI High	VIF
Intercept	89.45	1	1.64	85.58	93.32	
A-Voltage	-0.4312	1	1.29	-3.49	2.63	1.0000
B-Flow rate	-0.8087	1	1.29	-3.87	2.25	1.0000
C-Soluplus Conc	-4.29	1	1.29	-7.35	-1.23	1.0000
AB	3.78	1	1.83	-0.5526	8.11	1.0000
AC	-1.52	1	1.83	-5.85	2.82	1.0000
BC	0.3150	1	1.83	-4.02	4.65	1.0000
A^2	-14.08	1	1.78	-18.30	-9.86	1.01
B ²	-6.62	1	1.78	-10.84	-2.40	1.01
C ²	-2.80	1	1.78	-7.02	1.42	1.01

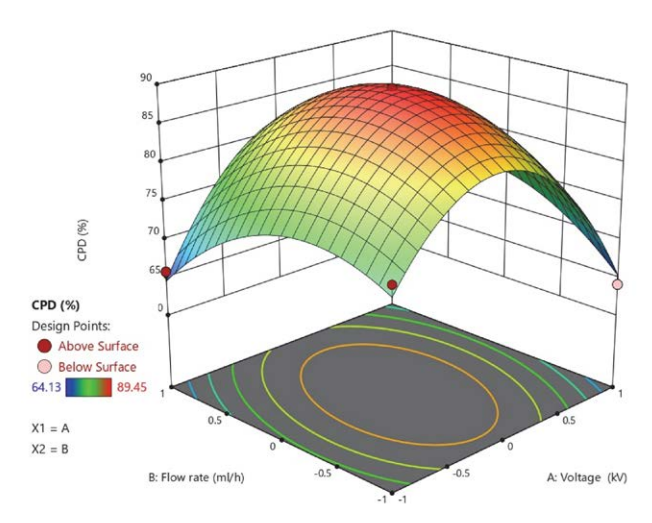


Figure 3. Three dimensional response plot of the experimental runs

3. 3. In Vitro Dissolution Studies

In the case of BCS II drug candidates such as efavirenz, dissolution is the rate-limiting step in oral absorption. An effective oral delivery strategy would be to improve the dissolution of the drug in such a situation. In this study, raw efavirenz (EFV) dissolution was found to be slow and incomplete (27.3 \pm 2.4%). Compared with native raw efavirenz (EFV), the dissolution profiles of the studied samples (Figs. 4 and 5) revealed that the nanofiber samples released the drug significantly faster (p < 0.05) than native raw efavirenz (EFV). The formulation F2 (EFV-NF) released the highest percentage of efavirenz (89.0 ± 3.2%) from the nanofiber samples which may be due to the amorphous state of the drug.6 We previously reported an improvement in dissolution when co-processing with hydrophilic polymers such as hydroxypropyl methylcellulose and polyvinyl pyrrolidone.³² The optimized formulation F2 (EFV-NF) was further subjected to other instrumental characterization.

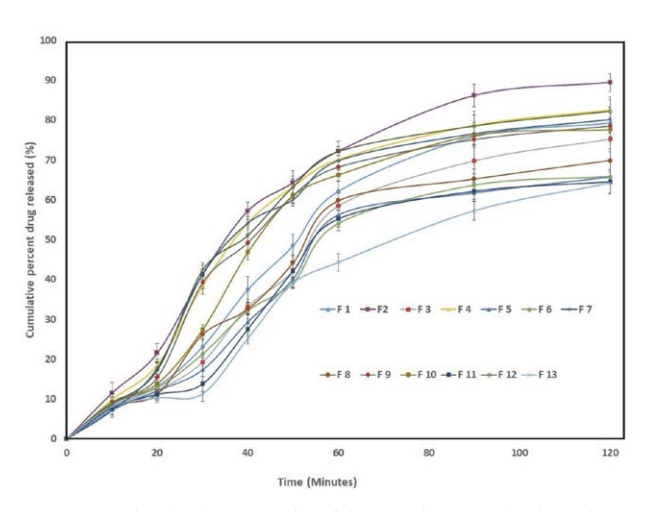


Figure 4. The dissolution profile of the nanofiber samples from the experimental runs.

3. 4. Scanning Electron Microscopic Investigation

An electron microscope is a powerful tool for observing the morphology and structure of a sample at a very high resolution. By coating the sample with gold, the sputter coater prevents charge build-up on the sample, which can distort images. This gold layer acts as a conductive layer on the sample. Focus depth and resolution are affected by the acceleration voltage used in the micrographs. Secondary electrons are detected by the Everhart-Thornley detector, which improves contrast and resolution. SEM confirmed the presence of nanofibers (Fig. 6). Inspecting the nanofibers (optimized nanofiber formulation i.e. EFV-NF and polymer-only nanofiber) with SEM revealed that their diameter ranged within 250-275 nm. The diameter of the nanofibers, particularly for EFV-NF, remained largely unaffected by drug loading. However, SEM analysis was not conducted for the other nanofiber formulations, preventing the reporting of additional findings for those variants. No crystals of the drug were visible on the SEM images of efavirenz-loaded nanofibers (D), indicating that the loaded efavirenz was dispersed molecularly in the polymer matrices. However, scanning electron microscopy (SEM) images of pure efavirenz showed a clear crystalline structure.

3. 5. X-ray Diffraction Studies

The prepared samples were analyzed by X-ray diffraction to assess whether any polymorphic transitions took place in efavirenz when formulated as nanofibers (EFV-NF). The X-ray diffraction patterns of native efavirenz, as a physical mixture with the matrix-forming polymer, and efavirenz-loaded nanofibers are depicted in Fig. 7. The XRD pattern of efavirenz alone (EFV) exhibited high-intensity peaks at diffraction angles 6.12°, 10.41°, 12.28°, 13.25°, 14.21°, 16.90°, 21.24°, and 24.90° (2θ) which revealed its crystalline nature. In contrast, efa-

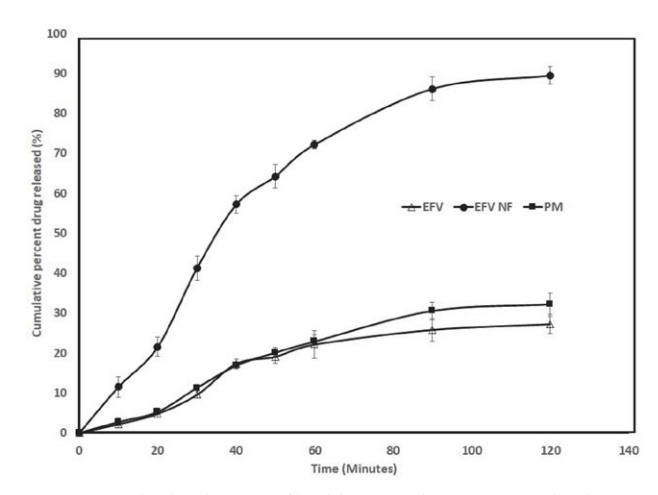


Figure 5. The dissolution profile of the naïve efavirenz (EFV), the physical mixture (PM), and the optimized nanofiber sample (EFV-NF).

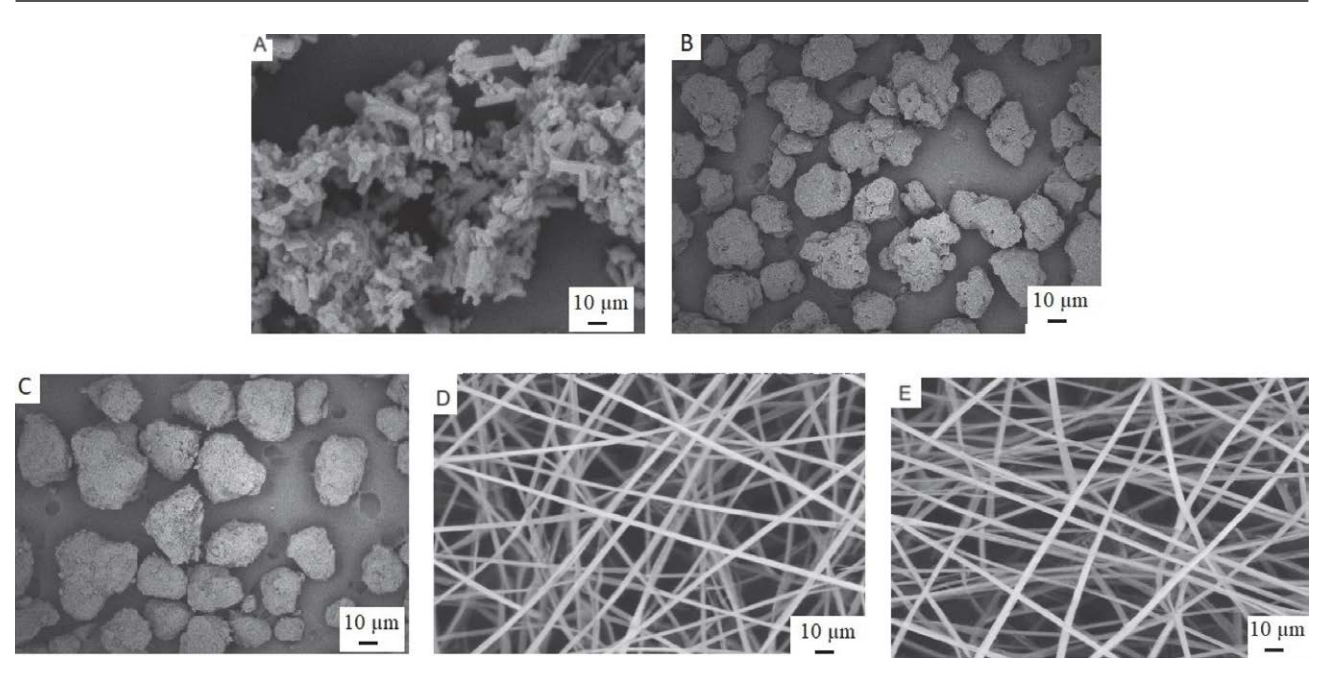


Figure 6. Scanning electron microscopic images of various samples. (A) native efavirenz, (B) Soluplus as received, (C) physical mixture of efavirenz and Soluplus, (D) efavirenz-loaded Soluplus nanofibers, and (E) Soluplus nanofibers.

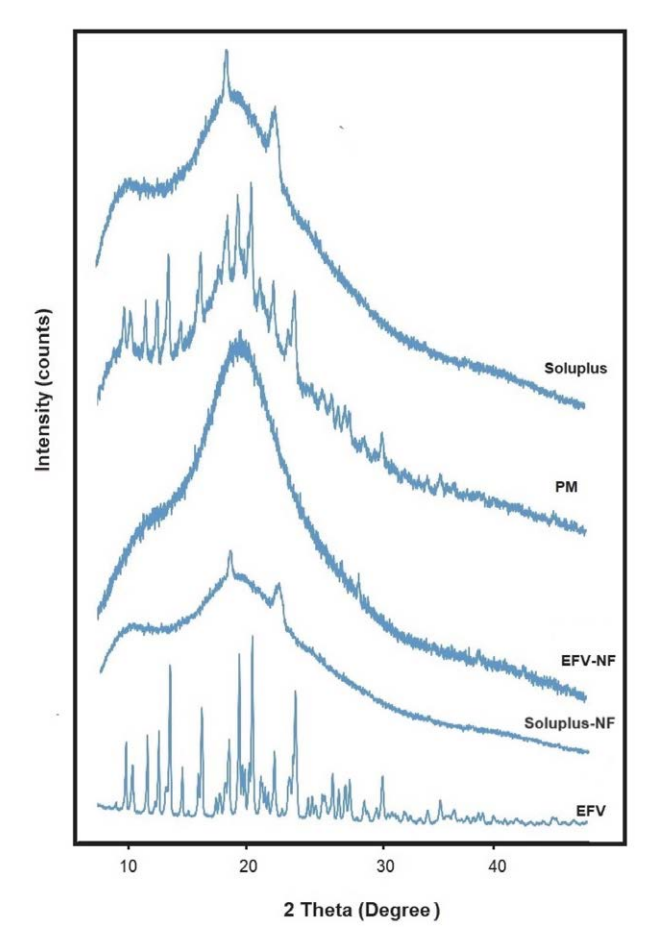


Figure 7. X-ray diffraction patterns of the studied samples indicated negligible or no crystallinity in the efavirenz-loaded nanofiber sample (EFV-NF). The raw efavirenz (EFV) and physical mixture (PM) samples retained the crystalline peaks.

virenz-loaded nanofibers showed broad and diffuse maxima, which may be attributed to efavirenz's amorphization here (EFV-NF). Efavirenz (PM) samples prepared by mixing efavirenz with Soluplus also retained their crystalline properties. Drug substances in the amorphous state possess many advantages over their crystalline counterparts, including improved solubility, wettability, and dissolution rate. ^{30,31}

3. 6. Differential Scanning Calorimetry (DSC)

As can be seen from Fig. 8, the DSC thermograms of samples correlate well with the XRD results. A sharp endothermic peak was identified for efavirenz alone (EFV) at 139.85 °C, the melting point of the drug, demonstrating its crystalline nature.³³ The physical mixture sample (PM) retained efavirenz's melting endotherm in the DSC studies. A small peak was observed in the nanofiber samples (EFV-NF) in association with the melting of the efavirenz, indicating its significant amorphization in the nanofiber samples (EFV-NF).³⁴ Thus, DSC studies agreed with the XRD analysis. This confirmed the amorphization of efavirenz in the electrospun nanofibers. The nanofibers thus presented an improved solubility and dissolution rate of efavirenz as observed in the in vitro studies.

4. Conclusion

QbD principles were efficiently applied to the development of efavirenz-loaded nanofibrous mats with enhanced dissolution. DSC and XRD results indicate the presence of efavirenz in an amorphous state in the nanofiber matrix. It

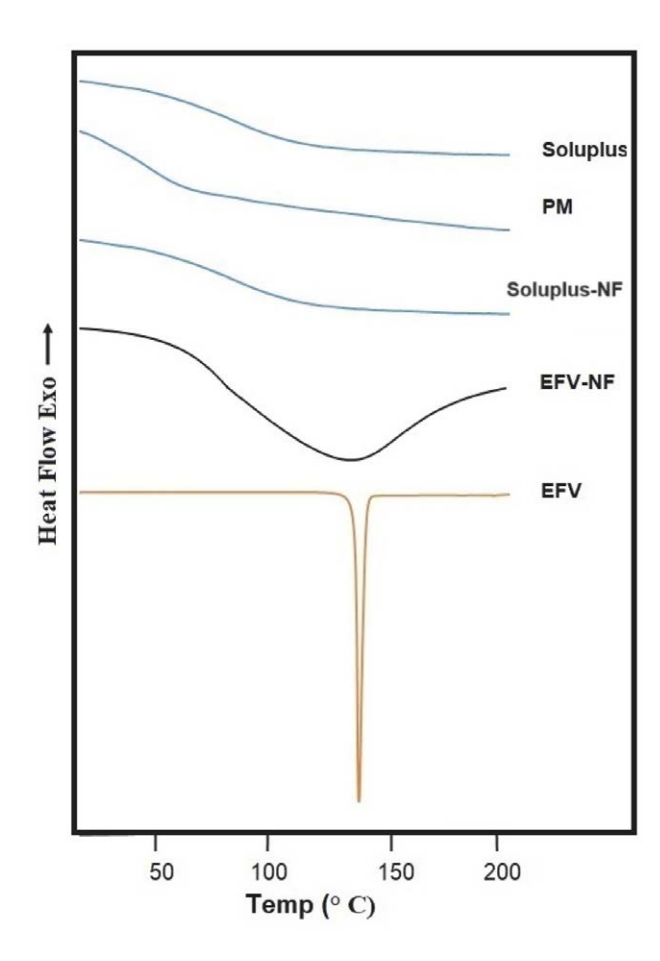


Figure 8. DSC thermograms of the studied samples indicate sharp melting endotherms at the melting point of efavirenz in raw efavirenz (Efavirenz) and physical mixture (PM) samples. Efavirenz-loaded nanofiber sample (EFV-NF) lacks a sharp endothermic peak.

is possible that Soluplus's antinucleating properties are responsible for the absence of crystalline efavirenz traces in the nanofiber samples. Further, a long-term stability study is planned to assess the shelf-life and storage conditions of the efavirenz-loaded nanofibrous mats. Additional preclinical studies are warranted based on the findings of the study. It appears that the nanofiber matrix provides a safe and effective environment for the delivery of amorphous efavirenz to the body. There is still a need for further research to assess its efficacy and safety in clinical trials.

Conflict of Interest

The authors declare no conflict of interest. The authors alone are responsible for the content and writing of the article.

Acknowledgment

The authors would like to acknowledge the financial support of All India Council for Technical Education

(AICTE), New Delhi, India, under Research Promotion Scheme [File No. 8-27/FDC/RPS (POLICY 1)/2019-20].

5. References

- D. Paul, G. Sanap, S. Shenoy, D. Kalyane, K. Kalia, R. K. Tekade, *Drug Discov. Today* **2021**, *26*, 80–93.
 DOI:10.1016/j.drudis.2020.10.010
- L. Tripathi, P. Kumar, K. Swain, S. Pattnaik, in *Drug Design Using Machine Learning*, ed. by Inamuddin, Tariq Altalhi, Jorddy N. Cruz, Moamen Salah El-Deen Refat, John Wiley & Sons, Ltd, New Jersey, 2022, pp. 143–164.
 DOI:10.1002/9781394167258.ch5
- 3. S. Mallick, S. Pattnaik, K. Swain, P. K. De, *Drug Dev. Ind. Pharm.* **2007**, *33*, 865–873. **DOI**:10.1080/03639040701429333
- 4. S. Pattnaik, K. Swain, J. V. Rao, V. Talla, K. B. Prusty, S. K. Subudhi, *RSC Adv.* **2015**, *5*, 74720–74725. **DOI**:10.1039/C5RA13038G
- S. Mallick, S. Pattnaik, K. Swain, P. K. De, A. Mondal, G. Ghoshal, A. Saha, *Drug Dev. Ind. Pharm.* 2007, *33*, 535–541.
 DOI:10.1080/03639040601050130
- S. Mallick, S. Pattnaik, K. Swain, P. K. De, A. Saha, G. Ghoshal,
 A. Mondal, Eur. J. Pharm. Biopharm. 2008, 68, 346–351.
 DOI:10.1016/j.ejpb.2007.06.003
- S. Mallick, S. Pattnaik, K. Swain, P. K. De, A. Saha, P. Mazumdar, G. Ghoshal, *Drug Dev. Ind. Pharm.* 2008, 34, 726–734.
 DOI:10.1080/03639040801901868
- 8. S. Pattnaik, K. Pathak, *Curr. Pharm. Des.* **2016**, *23*, 467–480. **DOI**:10.2174/1381612822666161026162005
- W. H. De Jong, P. J. Borm, Int. J. Nanomedicine 2008, 3, 133– 149. DOI:10.2147/IJN.S596
- S. Pattnaik, K. Swain, *Cellul. Chem. Technol.* 2022, 56, 115–122. DOI:10.35812/CelluloseChemTechnol.2022.56.10
- S. Pattnaik, K. Swain, S. Ramakrishna, Wiley Interdiscip. Rev. Nanomed. Nanobiotechnol. 2022. DOI:10.1002/wnan.1859
- 12. S. Pattnaik, K. Swain, Z. Lin, *J. Mater. Chem. B* **2016**, *4*, 7813–7831. **DOI:**10.1039/C6TB02086K
- S. S. Hota, S. Pattnaik, S. Mallick, Acta Chim. Slov. 2020, 67, 179–188. DOI:10.17344/acsi.2019.5311
- Y. C. Yadav, S. Pattnaik, K. Swain, Drug Dev. Ind. Pharm.
 2019, 45, 1889–1895. DOI:10.1080/03639045.2019.1672717
- D. S. Panda, N. K. Alruwaili, S. Pattnaik, K. Swain, *Acta Chim. Slov.* 2022, 69, 483–488. DOI:10.17344/acsi.2022.7370
- S. Pattnaik, K. Swain, J. V. Rao, T. Varun, K. B. Prusty, S. K. Subudhi, *RSC Adv.* **2015**, *5*, 91960–91965.
 DOI:10.1039/C5RA20411A
- S. Pattnaik, K. Swain, P. Manaswini, E. Divyavani, J. V. Rao,
 V. Talla, S. K. Subudhi, *J. Drug Deliv. Sci. Technol.* 2015, 29,
 199–209. DOI:10.1016/j.jddst.2015.07.021
- 18. A. Laha, S. Yadav, S. Majumdar, C. S. Sharma, *Biochem. Eng. J.* **2016**, *105*, 481–488. **DOI**:10.1016/j.bej.2015.11.001
- D. G. Yu, J. J. Li, G.R. Williams, M. Zhao, J. Control. Release 2018, 292, 91–110. DOI:10.1016/j.jconrel.2018.08.016
- B. Démuth, A. Farkas, B. Szabó, A. Balogh, B. Nagy, E. Vágó, et al., Adv. Powder Technol. 2017, 28, 1554–1563.

- DOI:10.1016/j.apt.2017.03.026
- H. E. Abdelhakim, A. Coupe, C. Tuleu, M. Edirisinghe,
 D.Q.M. Craig, *Mol. Pharm.* 2019, *16*, 2557–2568.
 DOI:10.1021/acs.molpharmaceut.9b00159
- 22. M. Basha, A. Salama, S. H. Noshi, *Drug Dev. Ind. Pharm.* **2020**, *46*, 253–263. **DOI:**10.1080/03639045.2020.1716376
- S. Nam, J. J. Lee, S. Y. Lee, J. Y. Jeong, W. S. Kang, H. J. Cho, Int. J. Pharm. 2017, 526, 225–234.
 DOI:10.1016/j.ijpharm.2017.05.004
- D. A. Chiappetta, C. Hocht, C. Taira, A. Sosnik, *Nanomedicine*. 2010, 5, 11–23. DOI:10.2217/nnm.09.90
- M. Patel, R. Shah, K. Sawant, Recent Pat. Nanotechnol. 2020, 14, 119–127. DOI:10.2174/1872210513666191019103129
- K. Swain, S. Pattnaik, N. Yeasmin, S. Mallick, Eur. J. Drug Metab. Pharmacokinet. 2011, 36, 237–241.
 DOI:10.1007/s13318-011-0053-x
- S. Pisani, I. Genta, R. Dorati, T. Modena, E. Chiesa, G. Bruni,
 M. Benazzo, B. Conti, J. Drug Deliv. Sci. Technol. 2022, 68,
 103060. DOI:10.1016/j.jddst.2021.103060

- 28. S. Pattnaik, K. Swain, A. Bindhani, S. Mallick, *Drug Dev. Ind. Pharm.* **2011**, *37*, 465–474.
 - **DOI:**10.3109/03639045.2010.522192
- K. Swain, S. Pattnaik, S. Mallick, K. A. Chowdary, *Pharm. Dev. Technol.* 2009, 14, 193–198.
 DOI:10.1080/10837450802498902
- 30. R. N. Kamble, P. P. Mehta, & A. Kumar, *AAPS PharmSciTech*. **2016**, *17*, 1240–1247. **DOI:**10.1208/s12249-015-0446-2
- 31. R. Laitinen, K. Löbmann, H. Grohganz, P. Priemel, C. J. Strachan, T. Rades, *Int. J. Pharm.* **2017**, *532*, 1–12. **DOI:**10.1016/j.ijpharm.2017.08.123
- 32. S. J. Dengale, H. Grohganz, T. Rades, K. Löbmann, *Adv. Drug Deliv. Rev.* **2016**, *100*, 116–125.
 - DOI:10.1016/j.addr.2015.12.009
- J. J. Moura Ramos, M. F. M. Piedade, H. P. Diogo, M. T. Viciosa, J. Pharm. Sci. 2019, 108, 1254–1263.
 - **DOI:**10.1016/j.xphs.2018.10.050
- 34. Z. M. M. Lavra, D. Pereira de Santana, M. I. Ré, *Drug Dev. Ind. Pharm.* 2017, 43, 42–54.
 - DOI:10.1080/03639045.2016.1205598

Povzetek

Slaba vodotopnost pogosto povzroči slabo raztapljanje in posledično slabo biološko uporabnost zdravil, katerih absorpcija v črevesju je omejena s hitrostjo raztapljanja. Farmacevtski tehnologi morajo opredeliti strategije za izboljšanje topnosti in hitrosti raztapljanja kandidatnih zdravil, da bi izboljšali njihovo biološko uporabnost. V pričujoči raziskavi so proučevali elektrostatsko sukanje polimernih nanovlaken z efavirenzom (protiretrovirusno zdravilo), zdravilo razreda II po biofarmacevtskem klasifikacijskem sistemu. Za izdelavo nanovlaken je bil uporabljen hidrofilni polimer, ki ga je mogoče elektrostatsko sukati, kot je Soluplus. Za optimizacijo parametrov elektrostatskega sukanja je bila uporabljena statistična zasnova eksperimentov. Študije s vrstično elektronsko mikroskopijo (SEM) so potrdile prisotnost nanovlaken. Študije rentgenske difrakcije (XRD) in diferenčne dinamične kalorimetrije (DSC) so potrdile amorfizacijo efavirenza v vzorcih nanovlaken. Optimizirana platforma na osnovi nanovlaken je v primerjavi s čistimi kristali efavirenza (27,3 \pm 2,4 %) znatno izboljšala in vitro raztapljanje efavirenza (89,0 \pm 3,2 % v 120 minutah).



Except when otherwise noted, articles in this journal are published under the terms and conditions of the Creative Commons Attribution 4.0 International License